as evidence against the requirement of ester hydrolysis before iron removal from enterobactin.

Biological Activity. Both the DHBS linear trimer and DHBS linear dimer are active as transport agents for radioactively labeled iron in whole *E. coli* RW193 cells. The initial rate of iron uptake from these compounds was essentially identical with the rate of enterobactin-mediated iron uptake when the pH of the uptake buffer was from pH 6 to 8 (Figure 8). The data in Figure 8 were derived from a series of uptake kinetics experiments by following the incorporation of ^{59}Fe–ligand complex into the cells and determining the initial rate. The lack of pH dependence on the uptake ratio indicates that the cell surface receptor is not sensitive to either bis(catecholate coordination (as in the Fe–DHBS linear dimer complex) or partially protonated tris(catecholate) coordination (as in the Fe linear trimer complex).

Summary

The stabilities of the ferric complexes of the stepwise hydrolysis products of enterobactin have been investigated. By comparison of the linear trimer (the first hydrolysis product of the cyclic trilactone enterobactin) with the parent compound, it is found that the exceptional stability of ferric enterobactin versus ferric complexes of tris(catechol) analogues is one-third enthalpic and two-thirds entropic in origin. Both the linear trimer and linear dimer hydrolysis products are effective iron uptake mediators when compared with enterobactin.

Acknowledgment. This research was supported by NIH Grant AI 11744. An American Cancer Society fellowship (to D.J.E.) is gratefully acknowledged.

Registry No. MECAMS, 71353-06-5; Fe, 7439-89-6; linear trimer, 30414-16-5; ferric linear trimer, 131685-07-9; linear dimer, 30414-15-4; ferric linear dimer, 131685-08-0; enterobactin, 28384-96-5; ferric enterobactin, 61481-53-6.

Supplementary Material Available: Figures S1–S3, showing a pH titration profile for the free linear trimer (**2**) and 1:1 mixtures of linear trimer and Fe^{3+}, UV/vis spectra of the linear dimer (**3**) titrated with ferric NTA, and UV/vis spectra of DHBS (**4**) titrated with ferric NTA (3 pages). Ordering information is given on any current masthead page.

Contribution from the Department of Chemistry, University of California, Berkeley, California 94720

Solution Equilibria of Enterobactin and Metal–Enterobactin Complexes[1]

Lawrence D. Loomis and Kenneth N. Raymond*

Received May 1, 1990

The solution thermodynamics of the siderophore enterobactin (ent), a powerful iron chelator, and of the synthetic analogue MECAM (*N,N',N''*-tris(2,3-dihydroxybenzoyl)-1,3,5-tris(aminomethyl)benzene) have been studied by UV spectrophotometry. Spectra were taken at high dilution by using a fully automatic, microcomputer-controlled spectrophotometer. The protonation constants for the *o*-hydroxyl groups of the ligand catechol moieties have been determined to be identical within experimental error: for L^{6-} to $LH_n^{(6-n)-}$, $\log K_6 = 6.0$ (5), $\log K_5 = 7.5$ (2), and $\log K_4 = 8.5$ (1). On the basis of these values, the overall protonation constant β_{016} for ent can be estimated as $10^{58.5}$, yielding a revised estimate for the formal stability constant of $[Fe(ent)^{3-}]$ of 10^{49}. The thermodynamic constants for protonation of the ferric complexes of ent and MECAM have been measured, for $Fe(L)^{3-}$ to $Fe(H_nL)^{(3-n)-} + nH$: for ent, $\log K_1 = 4.95$, $\log K_2 = 3.52$, and $\log K_3 = 2.5$; for MECAM, $\log K_1 = 7.2$, $\log K_2 = 6.03$, $\log K_3 = 4.5$, and $\log K_4 = 3.8$. Protonation takes place by discrete one-proton steps, consistent with a shift from catecholate binding to salicylate binding geometry upon protonation of the ligand *m*-hydroxyl groups. Protonation constants were also obtained for the complexes between ent and other trivalent metals: Sc^{3+}, Al^{3+}, Ga^{3+}, and In^{3+}. The order of protonation is (from highest pK_a to lowest) Al > Fe > Sc > Ga ≫ In. While $[Sc(ent)]^{3-}$ and $[Ga(ent)]^{3-}$ are similar to the ferric complexes and protonate in single proton steps, $Al(ent)^{3-}$ and $In(ent)^{3-}$ have mechanisms involving multiproton steps, possibly involving catecholate dissociation. This behavior was monitored by circular dichroism spectra.

Introduction

Iron is the most abundant transition metal found in the biosphere; it is required for almost all living organisms from hominids to bacteria.[2] In humans iron is of medical concern because of its effects on infectious organisms[3,4] and in diseases of iron deficiency and iron overload.[5,6] Current applications for iron-binding drugs include treatment of iron poisoning and of chronic iron overload associated with certain kinds of anemias.[5-7] Because iron in its most common form is not a readily available nutrient (the solubility of ferric hydroxide is 10^{-38},[8] strategies have been evolved by living organisms to acquire sufficient quantities of this vital metal. Many microorganisms, for example, produce siderophores—low molecular weight chelating agents that bind and solubilize ferric iron.[9-13] In part driven by clinical concerns, considerable research has taken place on the binding of iron by siderophores and by synthetic siderophore analogues. Of all the natural and man-made compounds so far investigated, the one that binds iron the most strongly under physiological conditions is a siderophore produced by *Escherichia coli*, enterobactin (ent) (Figure 1).[13-16]

Enterobactin employs three catechol (1,2-dihydroxybenzene) moieties to tightly encapsulate ferric iron in a hexadentate coordination sphere.[15-17] The overall reaction that defines the formal stability constant between enterobactin and trivalent metal ions, such as Fe^{3+}, is

$$M^{3+} + ent^{6-} = [M(ent)]^{3-} \quad \beta_{110} \qquad (1)$$

* To whom correspondence should be addressed.

(1) Coordination Chemistry of Microbial Iron Transport. 44. Previous paper: see ref 16.
(2) Lankford, C. *CRC Crit. Rev. Microbiol.* **1973**, *2*, 273.
(3) Weinberg, E. D. *Science* **1974**, *184*, 952.
(4) Jones, R. L.; Petersen, C. M.; Grady, R. W.; Kumbari, T.; Cerami, A.; Graziano, J. H. *Nature (London)* **1977**, *267*, 63.
(5) Anderson, W. F.; Hiller, M. C. U.S. Department of Health, Education and Welfare, Bethesda, MD, 1975, DHEW Publication No. 77-994.
(6) Anderson, W. F. In *Inorganic Chemistry in Biology and Medicine*; Martell, A. E., Ed.; ACS Symposium Series 140; American Chemical Society: Washington, DC, 1980; p 251.
(7) Raymond, K. N.; Harris, W. R.; Carrano, C. J.; Weitl, F. L. In *Inorganic Chemistry in Biology and Medicine*; Martell, A. E., Ed.; ACS Symposium Series 140; American Chemical Society: Washington, DC, 1980; p 314.
(8) Skoog, D. A.; West, D. M. *Fundamentals of Analytical Chemistry*, 3rd ed.; Holt, Reinhart, and Winston: New York, 1976.
(9) Raymond, K. N.; Müller, G.; Matzanke, B. F. In *Topics in Current Chemistry*; Boschke, F. L., Ed.; Springer-Verlag: Berlin, Heidelberg, 1984; Vol. 123, p 50.
(10) Neilands, J. B. *Annu. Rev. Nutr.* **1981**, *1*, 27.
(11) Hider, R. C. *Struct. Bonding* **1984**, *58*, 25.
(12) Matzanke, B. F.; Müller-Matzanke, G.; Raymond, K. N. In *Iron Carriers and Iron Proteins*; Loehr, T. M., Ed.; VCH Publishers: New York, 1989; p 1.

0020-1669/91/1330-0906$02.50/0

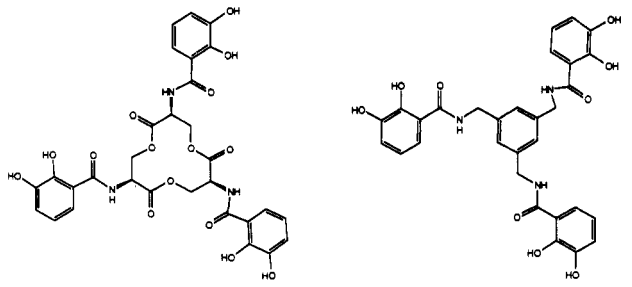

Enterobactin MECAM

Figure 1. Structural diagrams of enterobactin and its analogue MECAM.

Attempts to determine the formation constant for $[Fe(ent)]^{3-}$ potentiometrically have failed because the "titration is prematurely terminated at pH 3.8 by the precipitation of a purple complex."[18] A conditional formation constant, based on estimated protonation constants for ent, was obtained via competition with EDTA at pH 5.0. To convert the conditional constant into a conventional, proton-independent, formation constant, the six ligand protonation constants must be known:

$$\mathrm{ent^{6-} + H^+ \overset{K_1}{=} Hent^{5-} + H^+ \overset{K_2}{=} H_2ent^{4-} + H^+ \overset{K_3}{=} H_3ent^{3-} + H^+ \overset{K_4}{=} H_4ent^{2-} + H^+ \overset{K_5}{=} H_5ent^- + H^+ \overset{K_6}{=} H_6ent} \quad (2)$$

The protonation constants of ent have not been measured heretofore, because the backbone ring of ent incorporates ester linkages and is susceptible to acid- to base-catalyzed hydrolysis in aqueous solution;[18,19] furthermore, the fully protonated ligand is neutral and only slightly soluble in water. Values for those protonation constants have been estimated from model complexes such as *N,N*-dimethyl-2,3-dihydroxybenzamide (DMB). If the average value of the *o*-hydroxyl protonation constants of ent is assumed to be 8.4, the value determined for the ortho proton of DMB, and, similarly, 12.1 for the meta protons, then the overall protonation constant for $entH_6$ is estimated to be $\beta_{016} = 10^{61.5}$. The formation constant for iron binding was then estimated as $\beta_{110} = 10^{52}$. To better calculate metal formation constants, more accurate values for the ligand protonation constants were needed. The synthetic triscatechoylamide ligand MECAM (Figure 1) is a better model for ent than is DMB, since MECAM and ent have entirely secondary amide linkages, while DMB has a tertiary amide. Alkylation of the amide affects the values for the ligand protonation constants substantially.[20]

The composition and structure of protonated ferric enterobactin complexes have been the subject of some controversy and recently have been definitively probed by solution nuclear magnetic resonance studies.[21] In our model the hexadentate ML^{3-} complex protonates through one-proton steps until the purple MLH_3^0 complex precipitates:[18,21,22]

$$\mathrm{ML^{3-} + H^+ = MLH^{2-} + H^+ = MLH_2^- + H^+ = MLH_3^0(ppt)} \quad (3)$$

The observed precipitation has made analysis of the thermodynamic data difficult, because of the relatively high concentrations required for potentiometric titrations.[18] A similar problem has been observed with previous spectrophotometric titrations; the intensities of the ligand-to-metal charge-transfer bands observed in the visible spectra of these complexes are relatively low, and concentrations that are high enough to yield good spectra result in precipitation.

The thermodynamic properties of metal–enterobactin complexes have a pronounced effect on its biological function. The amount of available iron is linked to pathogenicity in these organisms.[3,4] The *E. coli* outer membrane receptor for ferric enterobactin differentiates between the complexes formed by ent with several trivalent metals—$[Fe(ent)]^{3-}$ and $[Ga(ent)]^{3-}$, for example.[23] If recognition at the *E. coli* outer membrane receptor were dependent on the protonation state of the metal complex, then differing thermodynamic constants between metal complexes could explain the difference in biological behavior.

We have previously measured the equilibrium constants associated with several sulfonated catechoylamide-containing ligands and the complexes they form with gallium by UV spectrophotometry.[20] Those studies relied on changes in ligand-localized absorbance bands in the UV: the molar extinctions of such bands are quite large. Similarly, metal complexes with hydroxypyridinone-containing compounds have been studied spectrophotometrically at high dilution.[24] High-intensity absorbances for ent, MECAM, and metal complexes of these ligands are available for spectroscopic examination. We describe here the measurement of the first three protonation constants of MECAM and ent using UV spectrophotometric titrations on solutions at high dilution. The measurements were performed with a fully automatic, microcomputer-controlled spectrophotometric titrator of custom design. Similar techniques were used to measure the protonation constants associated with the following metal–ligand systems: $Fe(MECAM)^{3-}$ and Fe-, Al-, Ga-, In-, and $Sc(ent)^{3-}$. The values obtained for $Fe(ent)^{3-}$ and $Fe(MECAM)^{3-}$ imply that they protonate by three successive one-proton steps, consistent with the protonation scheme previously proposed from thermodynamic studies (eq 3)[18,25] and with recent nuclear magnetic resonance studies.[21] A similar protonation pathway appears to be followed by the gallium and scandium complexes of enterobactin, while different protonation schemes are proposed for the aluminium and indium complexes.

Experimental Section

Materials. MECAM (Figure 1) was synthesized as previously described.[26,27] Enterobactin (ent) was isolated from cultures of *E. coli* AN311 as previously described.[28] The following compounds were obtained from commercial sources: scandium trichloride (Aldrich); indium chloride tetrahydrate (Alfa); ferric chloride hexahydrate (Mallinckrodt); $^{59}FeCl_3$ and $^{55}FeCl_3$ (New England Nuclear); gallium and aluminum, as the pure metals (J. T. Baker). Fisher reagent grade KCl was passed down a CHELEX 100 column (100–200 mesh, K^+ form) to reduce iron contamination; this procedure was particularly important for the titrations of the ligands alone. Buffers were obtained from Calbiochem: MES = *N*-morpholineethanesulfonic acid, $pK_a = 6.15$; BIS–TRIS = (bis(2-hydroxyethyl)amino)tris(hydroxymethyl)methane, $pK_a = 6.46$; HEPES = *N*-(2-hydroxyethyl)piperazine-*N'*-ethanesulfonic acid, $pK_a = 7.55$. Metal solutions were prepared by dissolving the metal in acid and

(13) Loomis, L. D.; Stack, T. D. P.; Raymond, K. N. Enterobactin: Coordination Chemistry and Microbial Iron Uptake Studies. To be submitted to *Acc. Chem. Res.*
(14) Raymond, K. N.; Carrano, C. J. *Acc. Chem. Res.* **1979**, *12*, 183.
(15) Isied, S. I.; Kuo, G.; Raymond, K. N. *J. Am. Chem. Soc.* **1976**, *98*, 1763.
(16) Scarrow, R. C.; Ecker, D. J.; Ng, C.; Liu, S.; Raymond, K. N. Iron(III) Coordination Chemistry of Linear Dihydroxyserine Compounds Derived from Enterobactin. *Inorg. Chem.*, preceding paper in this issue.
(17) McArdle, J. V.; Sofen, S. R.; Cooper, S. R.; Raymond, K. N. *Inorg. Chem.* **1978**, *17*, 3075.
(18) Harris, W. R.; Carrano, C. J.; Cooper, S. R.; Sofen, S. R.; Avdeef, A. A.; McArdle, J. V.; Raymond, K. N. *J. Am. Chem. Soc.* **1979**, *101*, 6097.
(19) Greenwood, K. T.; Luke, R. K. J. *Biochim. Biophys. Acta* **1978**, *525*, 209.
(20) Loomis, L. D.; Raymond, K. N. Kinetics of Gallium Removal from Transferrin and Thermodynamics of Gallium-Binding by Sulfonated Tricatechol Ligands. *J. Coord. Chem.*, in press.
(21) Cass, M. E.; Garrett, T. M.; Raymond, K. N. *J. Am. Chem. Soc.* **1989**, *111*, 1677.
(22) Harris, W. R.; Raymond, K. N. *J. Am. Chem. Soc.* **1979**, *101*, 6534.
(23) Ecker, D. J.; Loomis, L. D.; Cass, M. E.; Raymond, K. N. *J. Am. Chem. Soc.* **1988**, *110*, 2457.
(24) Scarrow, R. C.; Riley, P. E.; Abu-dari, K.; White, D. L.; Raymond, K. N. *Inorg. Chem.* **1985**, *24*, 954.
(25) Harris, W. R.; Carrano, C. J.; Raymond, K. N. *J. Am. Chem. Soc.* **1979**, *101*, 2213.
(26) Weitl, F. L.; Raymond, K. N. *J. Am. Chem. Soc.* **1979**, *101*, 2728.
(27) Weitl, F. L.; Harris, W. R.; Raymond, K. N. *J. Med. Chem.* **1979**, *22*, 1281.
(28) Cooper, S. R.; McArdle, J. V.; Raymond, K. N. *Proc. Natl. Acad. Sci. U.S.A.* **1978**, *75*, 3551.

diluting to the desired concentration with distilled, deionized water. They were standardized by titrations with EDTA according to the methods of Welcher.[29]

Physical Techniques. Ultraviolet and visible (UV–vis) spectra were measured on a Hewlett-Packard 8450A spectrophotometer. Circular dichroism (CD) spectra were obtained on a JASCO J-500C spectropolarimeter with a DP-500N data processor. Electrophoresis was performed with a Savant TLE-20 thin-layer tank with a Bio-Rad 3000/300 power supply. Samples were streaked on Whatman 3-mm paper and run in 0.05 M HEPES buffer, pH 7.4.

Titration Procedure. Titrations were carried out by using a locally constructed microcomputer-controlled, automatic spectrophotometric titration apparatus. The instruments used included a Corning 130 pH meter, Sergeant-Welsh automatic buret, and a Hewlett-Packard 8450A UV–vis spectrophotometer including peripheral devices; the titration was controlled by a Commodore Pet 2001 personal computer with a locally constructed memory extension board. The software to run the titration was written to control two different configurations, either a 1-cm-path or 10-cm-path titration. The 1-cm-path titrations were run at higher concentration in a cuvette with a titration reservoir built onto the top. The 10-cm-path titrations were run in a locally constructed flow cell that fit in the spectrophotometer and was attached to a 50-mL-capacity temperature-jacketed reservoir.

Solutions to be titrated were made up as follows: 0.1 M KCl, to maintain ionic strength; 20–500 μM metal for titrations at 1-cm path and 1.5–10 μM for 10-cm titrations, from a stock solution in acid; stoichiometric, or slight excess, ligand from a stock solution in MeOH; 10- to 50-fold excess of buffer; distilled, deionized water to a total volume of 5 mL for the short path length titrations and 50 mL for the long path. Ligand solutions were calibrated spectrophotometrically; the molar extinction coefficient of both $entH_6$ and $MECAMH_6$ is 9500 at 316 nm.[16] Although the buffers used were not completely transparent in the region of interest, their relative molar extinction coefficients were sufficiently small compared to the ligands that they could be used with impunity at excesses under about 100-fold. Solutions were transferred to a cuvette in the spectrophotometer and a pH probe and buret tip placed into the titration reservoir. The solutions were mixed by sparging with water-saturated argon and with a cuvette stir bar with the Hewlett-Packard temperature controller/stirrer (1-cm cell only). Temperature was maintained at 25 °C throughout the titration, either with the Hewlett-Packard temperature controller or with an external constant-temperature circulating bath. The pH electrode was calibrated for hydrogen ion concentration (rather than activity) with standard solutions of acid and base prepared from Baker Dilut-It. The pH was adjusted in small increments by addition of either 1 N HCl or KOH. Points were taken at approximately 0.1 pH increments, a given titration included from 40 to 120 points.

The controlling programs for these titrations were menu-driven and allowed user interaction before and during the course of the titration. The following functions were controlled automatically: titrant delivery and adjustment of titrant volume to maintain a constant pH change between points; control of mixing by mechanical stirring and argon sparging; calibration of the pH meter and measurement of $p[H^+]$; approach to equilibrium for each point in the titration based both on changes in pH and in absorbance; storage of $p[H^+]$, spectrum, and volume of titrant for each point on floppy disk and cassette tape. Copies of the most recent versions of the programs used are available from the authors.

Results

MECAM and ent. The titration of MECAM from pH 5 to 10 is shown in Figure 2. The initial absorbance at high energy shifts to low energy as the pH is raised; the intensity of this peak increases upon deprotonation. MECAM was titrated both from low to high pH and from high to low pH. A small amount of precipitation was observed at low pH, shown by an increasing absorbance at 400 nm due to scattering. This precipitation was reduced significantly by addition of 5% MeOH and by titration from high pH to low. Enterobactin was titrated only from low to high pH, to avoid base-catalyzed hydrolysis. The pH-dependent spectra of ent were indistinguishable from those obtained in the MECAM titration.

$Fe(MECAM)^{3-}$ and $Fe(ent)^{3-}$. Precipitation was observed when $[Fe(ent)]^{3-}$ or $[Fe(MECAM)]^{3-}$ was titrated at a concentration greater than 50 μM, consistent with earlier observations.[18,22]

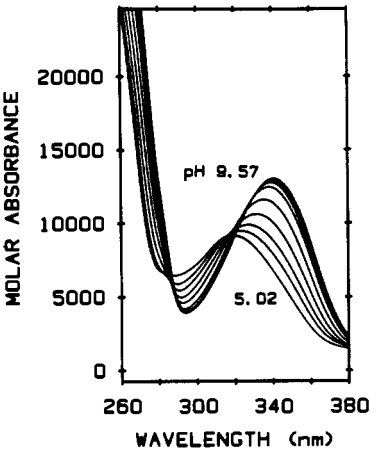

Figure 2. Spectrophotometric titration of MECAM (Figure 1). Conditions: [MECAM] = 1.67 μM; path = 10 cm; 5% MeOH by volume. The spectra shown were taken every 0.5 pH unit from about 5.0 to 9.5 (except for 9.0).

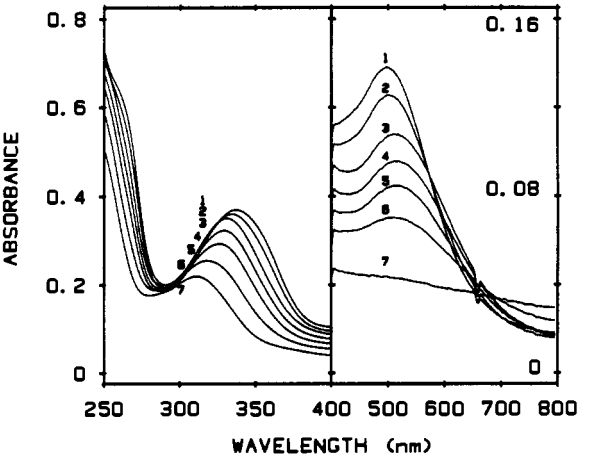

Figure 3. Spectrophotometric titration of Fe(ent). Conditions: [Fe] = 2.44 μM; [ent] = 2.50 μM; [Bis–Tris buffer] = 1 mM; 10-cm path. Approximately 15% of the data are shown: 1 (pH 6.10); 2 (5.06); 3 (4.07); 4 (3.57); 5 (3.06); 6 (2.57); 7 (2.08). Spectra are corrected for dilution but not for baseline shifts.

Complexes of $Fe[(MECAM)]^{3-}$ and $[Fe(ent)]^{3-}$ were titrated at high dilution, by monitoring the spectral changes in a 10 cm path length cuvette. At high pH, two bands were observed (Figure 3) for $[Fe(ent)]^{3-}$; in the UV region, λ_{max} = 337 nm (ϵ = 15 500 M^{-1} cm^{-1}), and in the visible region, λ_{max} = 498 (6000). At low pH, the band in the UV region shifted to 309 nm (7000), while the visible absorbance disappeared entirely. Isosbestic points were observed in the high-pH regime at 574 and 325 nm. At these extremely low concentrations no evidence for precipitation was observed at low pH.

$[M(ent)]^{3-}$. Complexes of ent with metal cations (Al^{3+}, Ga^{3+}, In^{3+}, and Sc^{3+}) were titrated at both high dilution (2–5 μM) and low (20–100 μM). At higher concentrations, precipitation was observed in the titrations of the gallium and scandium complexes. At low concentration, both these complexes displayed a maximum at 345 nm (14 500) at high pH; at low pH a shoulder near 310 nm (7500) was observed as well as an intense absorbance at higher energy. [This intense peak may be due to some degradation of the ligand at low pH.] Surprisingly, no precipitation was observed for the aluminum or indium complexes. An isosbestic point was observed in the high-pH spectra of all the metal–enterobactin complexes near 331 nm. The absorbances in the $[Al(ent)]^{3-}$ system shifted smoothly from a maximum at 344 nm (13 000) at pH 6.5 and above to a lower intensity maximum at 312 nm (7000) below about pH 2.0; similar results were obtained for $[In(ent)]^{3-}$. No spectral changes were observed above pH 6.5 or below pH 2.0.

Schwarzenbach Analysis. The data for the metal complexes with ent were examined by using the Schwarzenbach method.[30]

(29) Welcher, F. J. *The Analytical Uses of Ethylenediamine Tetraacetic Acid*; D. van Nostrand Co., Inc.: Princeton, NJ, 1958.

Table I. Properties of Enterobactin and MECAM as Functions of the Protonation State

ligand	protonation consts[a]				spectral properties[c]			
	K_6	K_5	K_4	av $[N]^b$	LH_6	LH_5	LH_4	LH_3
ent	6.0 (5)	7.5 (2)	8.55 (9)	7.36 [4]	313 (12.3)	341 (13.7)	344 (15.7)	345 (16.6)
MECAM	5.9 (5)	7.4 (2)	8.4 (1)	7.23 [5]	317 (10.0)	325 (11.1)	340 (15.0)	342 (15.4)

[a] Log values. Numbers in parentheses represent the standard deviation in the last significant digit. [b] $[N]$ is the number of duplicate data sets. [c] Wavelength at the absorption maximum, nm (molar extinction, M^{-1} cm^{-1}).

Table II. Thermodynamic and Spectroscopic Properties of Complexes between Enterobactin and Trivalent Metals

metal	ionic radius, Å[a]	log K_1	log K_2	log K_3	log K_4	spectroscopic properties: λ, nm (ε, M^{-1}, cm^{-1}) ML	MLH	MLH_2	MLH_3	MLH_4
Al	0.54	5.15	3.4		2.6[b]	346 (14.2)	343 (13.5)	333 (12.3)		311 (7.9)
Ga	0.62	4.53	3.71	2.5		346 (14.4)	336 (12.8)	333 (12.8)	303 (8.9)	
Fe	0.64	4.95	3.52	2.5		338 (15.1)	332 (14.7)	325 (11.9)	305 (9.0)	
		[4.89][c]	[3.15]			498 (5.7)	514 (4.6)	518 (3.5)	700 (1.7)	
Sc	0.74	4.67	3.84	3.31		345 (13.0)	337 (11.2)	334 (12.0)		
In	0.80	4.02			3.1[b]	344 (15.7)	332 (13.4)			311 (8.9)
Fe–MECAM		7.2	6.03	4.5	3.8	344 (12.7)	332 (13.1)	329 (12.5)	315 (11.0)	308 (11.1)
		[7.08]	[5.60]							

[a] From ref 36. [b] Multiple-proton steps. [c] Brackets: values from ref 23.

The high-pH data for each titration had an isosbestic point; absorbance functions from the spectra that passed through these points were plotted by assuming proton stoichiometries from 1 to 3. In every case, the plots of A(obs) vs $[A(\text{initial}) - A(\text{obs})]/[H^+]^n$ were linear only when a one-proton step ($n = 1$) was assumed. The following protonation constants (log values) were obtained: $[Fe(ent)]^{3-}$, 4.90 (5); $[Al(ent)]^{3-}$, 5.12 (5); $[Ga(ent)]^{3-}$, 4.5 (1); $[In(ent)]^{3-}$, 3.93 (5); $[Sc(ent)]^{3-}$, 4.6 (1); the value in parentheses represents the standard deviation in the last significant digit.

REFSPEC. On the basis of previous work on catechoylamide-containing ligand systems, the equilibrium constants of the ligand protonations were expected to overlap to a great extent.[20] Since no isosbestic points were apparent in the absorbance spectra, no attempt was made to analyze the titration data by simple methods. Instead, factor analyses and nonlinear least-squares methods were applied by using the program REFSPEC.[31,32] The model used to analyze the data included three protonation constants, K_6, K_5, and K_4, relating four absorbing species: LH_6, LH_5^-, LH_4^{2-}, and LH_3^{3-}. The deprotonation of the *m*-hydroxyls were assumed to be well-separated from the lower pH set. Refinements were obtained both for ent and MECAM; the fits of the calculated to observed spectra were very good except near pH 5.0. [At this pH there may have been a small amount of precipitation affecting the analysis. If the value obtained for K_6 is affected by precipitation, the true value is probably somewhat higher than that presented. The other protonation constants would not be affected by this.] A small amount of iron contamination was observed in the spectra; this accounted for less than 5% of the ligand, assuming ε(490 nm) = 6000 for $Fe(ent)^{3-}$. Including this small amount of Fe–L in the refinement caused no change in the calculated constants. The values obtained for the protonation constants of the ortho protons of ent and MECAM are summarized in Table I. These values for the two ligands are essentially identical. The species distribution curves and the calculated extinction coefficient spectra of the intermediate species obtained for ent are shown in Figure 4.

The metal titrations were also analyzed by nonlinear least-squares methods. Since the bulk properties of the metal–ligand complexes showed two kinds of behavior, two models were necessary. One model was found suitable to describe the behavior of metal complexes that precipitated at higher concentration: $[Fe(MECAM)]^{3-}$, $[Fe(ent)]^{3-}$, $[Ga(ent)]^{3-}$, and $[Sc(ent)]^{3-}$. The

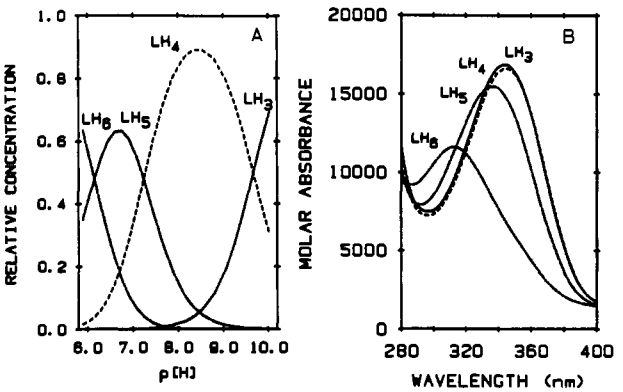

Figure 4. (A) Calculated species distribution and (B) extinction coefficient spectra for enterobactin at pH 10.0: (—) LH_3; (- - -) LH_4; (-·-) LH_5; (-··-) LH_6.

remaining two systems required a model that explained the lack of precipitation observed.

The model we have previously proposed for the protonation of the $[Fe(ent)]^{3-}$ complex (eq 3) was found to describe adequately the observed spectral properties. This was used for the Fe, Ga, and Sc complexes of ent. The $[Fe(MECAM)]^{3-}$ complex began to protonate at substantially higher pH than the $M(ent)^{3-}$ complexes, and another species, MLH_4, was implied and included in the model at low pH for this complex. In the refinements, the following species were included: the four absorbing M–L complexes (five for $[Fe(MECAM)]^{3-}$); LH_6 and LH_5 (the absorption spectra of which were fixed to the values obtained in the ligand-only titrations); the metal hydrolysis products, which do not absorb appreciably and whose equilibrium constants were fixed to reported values.[33] The four-component fit to the spectra for $[Fe(ent)]^{3-}$ was excellent for three of the four components and good for the fourth (see the supplementary material, Figure S1). Similar fits of calculated to observed components were obtained for the gallium and scandium complexes. No other model gave nearly as good a fit for any of these systems. The five-component fit to the data for $[Fe(MECAM)]^{3-}$ was also good.

A different model was necessary for the remaining two systems. Since complexes of these metals do not precipitate at low pH, it seemed unlikely that MLH_3^0 was an important species at any point during the titration. Although no potentiometric studies of the complexes of ent with these metals have been made, high-voltage paper electrophoresis showed the overall charge on the high-pH

(30) Anderegg, G.; L'Eplattenier, F.; Schwarzenbach, G. *Helv. Chim. Acta* **1963**, *46*, 1400.
(31) Scarrow, R. C. Hydroxypyridinones: Ligands with High Affinity for Iron(III). Ph.D. Dissertation, 1985, Department of Chemistry, University of California, Berkeley, CA.
(32) Turowski, P. N.; Rodgers, S. J.; Scarrow, R. C.; Raymond, K. N. *Inorg. Chem.* **1988**, *27*, 474.
(33) Smith, R. M.; Martell, A. E. *Critical Stability Constants*; Plenum Press: New York and London, 1976; Vol. 4.

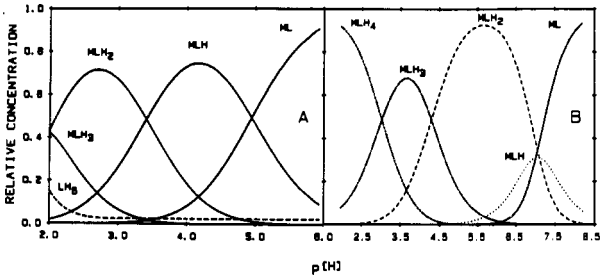

Figure 5. Calculated species distribution for ferric complexes of (A) ent (L = ent^{6-}) and (B) MECAM (L = $MECAM^{6-}$). Metal-containing species are normalized to the total concentration of iron. In (A) LH_6 (---) is normalized to total ligand concentration, which is in 2.5% excess over metal.

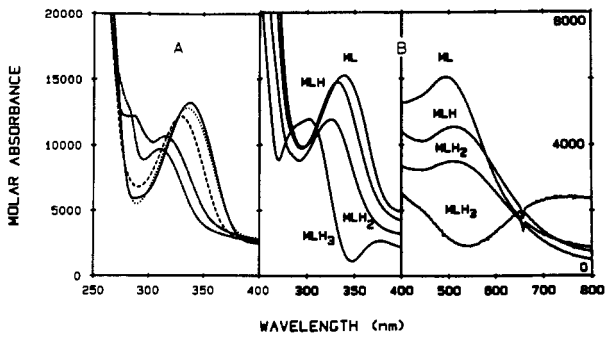

Figure 6. Calculated extinction coefficient spectra for (A) Fe(MECAM)$^{3-}$ and protonated Fe(MECAM)H_N complexes (N = 0 (—), N = 1 (···), N = 2 (- - -), N = 3 (-·-), N = 4 (-·--)) and (B) Fe(ent)$^{3-}$ and protonated Fe(ent)H_N complexes (note the different scale for the left panel relative to the center and right panels).

complexes to be −3. Similar, but not identical, models were found to describe the two systems. In the [Al(ent)]$^{3-}$ case, the following model was used:

$$ML^{3-} + H^+ = MLH^{2-} + H^+ = MLH_2^- + 2H^+ = MLH_4^+ \quad (4)$$

For In(ent)$^{3-}$, the MLH_2 species was not necessary to describe the data. The fits to the two models can be found in the supplementary material Figures S2 and S3. In no case would the [Al(ent)]$^{3-}$ system refine if the MLH_2 species was left out of the model, even though that species is never in very high concentration; similarly, adding MLH_2 to the indium system led to divergence in the refinement.

The thermodynamic constants obtained from these refinements are summarized in Table II. There was insufficient dissociation of metal–ligand complex observed to determine the formation constants. The overall formation constant, β_{110}, was fixed to the value estimated for [Fe(ent)]$^{3-}$. The species distributions predicted by using the obtained protonation constants for [Fe(ent)]$^{3-}$ and [Fe(MECAM)]$^{3-}$ are shown in Figure 5. In addition to refinement of the thermodynamic constants, extinction coefficient spectra for the species predicted to be in solution were calculated (Figure 6). The values for the peak maxima calculated for the various species are summarized in Table II.

In(ent)$^{3-}$. The model used for the indium complex resulted in the species distribution and extinction coefficient spectrum shown in Figure 7. Since this model was substantially different from that of the other systems, another spectroscopic technique was used to investigate it. Figure 8 shows the titration of [In(ent)]$^{3-}$ using circular dichroism (CD) as well as UV absorbance spectroscopy. At high pH the In(ent)$^{3-}$ complex showed a positive absorbance associated with the near-UV band, λ_{max} = 335 nm, $\Delta\epsilon$ = +7.38, similar to those previously obtained for the fully deprotonated [Fe(ent)]$^{3-}$ complex.[16] As the acidity was lowered to pH 3.5, the intensity of this peak decreased and a shoulder to low energy formed. Abruptly, between pH 3.5 and 3.0, this peak vanished and was replaced by a negative absorbance with λ_{min} = 292, $\Delta\epsilon$ = −5.61.

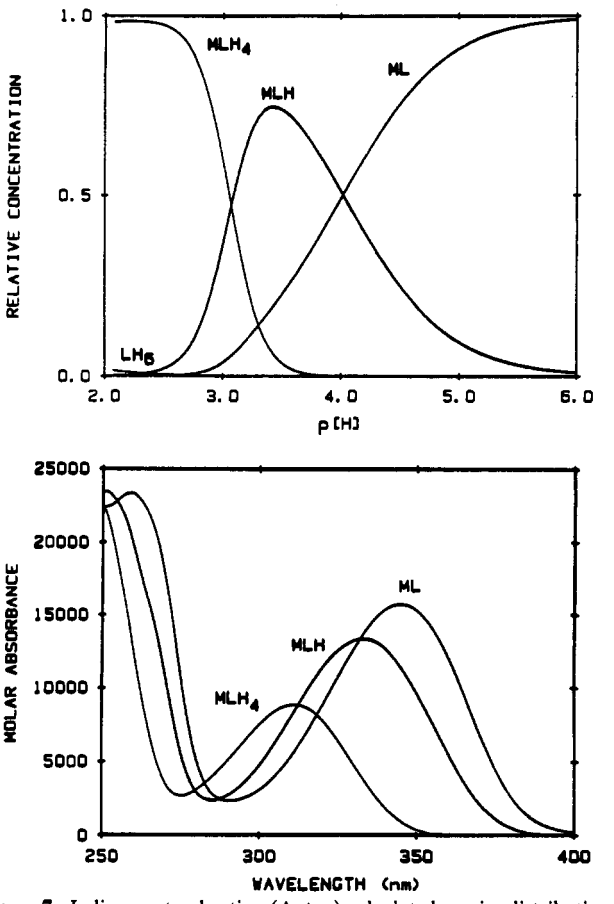

Figure 7. Indium–enterobactin: (A, top) calculated species distribution; (B, bottom) calculated extinction coefficient spectra.

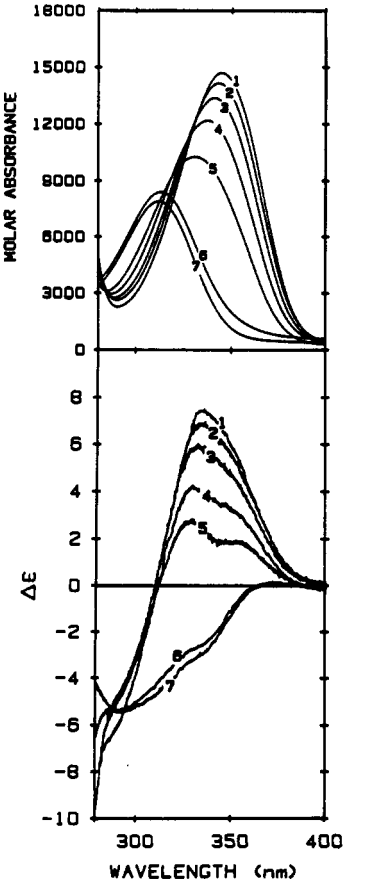

Figure 8. Titration of In(ent) for absorbance and CD spectra [spectrum no. (pH)]: 1 (6.5); 2 (5.0); 3 (4.5); 4 (4.0); 5 (3.5); 6 (3.0); 7 (2.5).

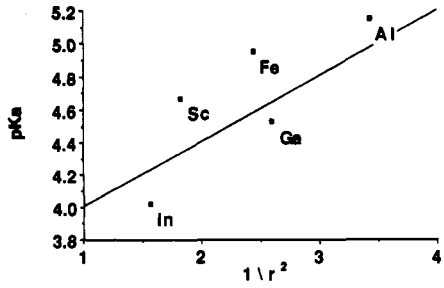

Figure 9. Plot of the first protonation constant for M(ent) complexes vs the charge density on the metal for M = Fe^{3+}, Al^{3+}, Ga^{3+}, In^{3+}, and Sc^{3+}. Ionic radii are from ref 36.

Discussion

Ligands. The similarity between the values obtained for the *o*-hydroxyl protonation constants of ent and MECAM indicates that MECAM is an excellent synthetic model ligand for ent. The average pK_a's of ent and MECAM are a full pH unit lower than predicted by the DMB model. This is consistent with results obtained with other catechoylamide systems in which measurements have been made on ligands that are identical except for substitution at the amide. For example, the difference between the average protonation constant (log values) of the ortho protons of MECAMS (an analogue of MECAM in which the catechol rings are sulfonated at the 4-position) and Me_3MECAMS (the same as MECAMS except that the amide nitrogens are methylated) is 0.6.[20] This can be attributed to the donation of electron density by the alkyl substituent on the amide to the hydroxyl oxygen. Although the base-catalyzed hydrolysis of ent is known to be fast above pH 10,[16,17] MECAM is not susceptible to hydrolysis. Until such measurements are made, the best estimate for log β_{016}, for ent and MECAM is 58.5. Using this value to revise the formal formation constant for $[Fe(ent)]^{3-}$ yields $\beta_{110} = 10^{49}$.

Metal Protonation Constants. The values obtained previously for the upper two protonation constants for $[Fe(ent)]^{3-}$ and $[Fe(MECAM)]^{3-}$ are shown in Table II along with the values obtained in this work. The agreement is very good for pK_1 and less good for pK_2. The depression of the calculated values for the protonation constants obtained previously is attributed to the presence of precipitate in those experiments. At constant pH, decreasing the amount of the more protonated species by precipitation will result in apparent depression of the observed pK_a.

For all of the systems studied, the ML^{3-} species first undergoes a single-proton step. The basicities of these metal complexes are expected to be related to the charge density (z/r^2) on the metal. Since these metals are all in the +3 oxidation state, z is a constant, and their charge densities are simply proportional to $1/r^2$, where r is the ionic radius. However, the relationship between log K and charge density (Figure 9) is not uniformly linear.

The $[Fe(ent)]^{3-}$ and $[Fe(MECAM)]^{3-}$ complexes protonate strictly by successive one-proton steps, with the separation between each pK_a on the order of a full pH unit or greater, and conform with the salicylate shift model.[18,21,22] Ga^{3+} and Sc^{3+} are similar, although the apparent degradation of the ligand in these two systems makes the choice of model less certain.

On the other hand, the Al- and In-ent systems exhibit significantly different protonation phenomena. They appear to include a two- and a three-proton step, respectively. Since the neutral (and less soluble) MLH_3 species are not present in significant amounts for these metal ions, spectroscopic studies can be carried out on quite concentrated solutions. The CD study of $[In(ent)]^{3-}$ is an example. The shoulder that grows in as the pH is lowered from 6.0 to 3.5 is consistent with two different chromophores being present. Over the course of a very small pH range (0.5 pH unit) the CD signal changes dramatically, consistent with the proposed model.

The models for the aluminum and indium complexes (the smallest and largest metals studied, respectively) include simultaneous protonations, whereas all of the other metals protonate via successive one-proton steps. From CPK models it seems that the salicylate-bonded mode is somewhat more strained than the catecholate mode. Possibly the strain on the MLH_3 salicylate species is sufficient that only metals within a fairly narrow ionic radius range can support that structure. Metals outside of that range, both larger (In) and smaller (Al), may avoid the strained complex by dissociative pathways.

Biological Recognition. Addition of excess $[Al(ent)]^{3-}$ or $[Ga(ent)]^{3-}$ to *E. coli* cultures does not significantly inhibit the uptake of $[Fe(ent)]^{3-}$, whereas $[In(ent)]^{3-}$, $[Sc(ent)]^{3-}$, and $[Rh(MECAM)]^{3-}$ do inhibit uptake.[23] Significant amounts of radiolabeled $[Sc(ent)]^{3-}$ are taken up by *E. coli*,[34] whereas very little $[Ga(ent)]^{3-}$ passes into the cells.[35] While Al^{3+} and Ga^{3+} are smaller than Fe^{3+} (Ga^{3+} only slightly so) and all the rest of the metals studied are larger, no physical property yet observed follows that trend. Recent work seems to exclude kinetics of exchange as a viable mechanism for separating these metals,[23] and the work described here would seem to exclude protonation behavior as a mechanism; redox behavior seems unlikely, and no other physical property is immediately apparent. In short, *E. coli* seems to distinguish between enterobactin complexes of iron and other common metals by a process we still cannot fully explain, even though this study has quantitatively characterized the differences in solution complexation and protonation behavior of those complexes.

Acknowledgment. We thank Dr. R. C. Scarrow for his contribution to the titration-controlling program and for the data analysis program REFSPEC. This research is supported by NIH Grant AI11744.

Registry No. MECAM, 69146-59-4; $Al(ent)^{3-}$, 113351-94-3; $Ga(ent)^{3-}$, 113351-93-2; $Fe(ent)^{3-}$, 61481-53-6; $Sc(ent)^{3-}$, 113429-11-1; $In(ent)^{3-}$, 113351-95-4; $Fe(MECAM)^{3-}$, 69058-77-1; enterobactin, 28384-96-5.

Supplementary Material Available: Figures S1–S3, showing the fit of the calculated spectra to those observed for the titration of Fe(ent), as a function of p[H], the fit to the component spectra for Al(ent), and the fit to the component spectra for In(ent) (4 pages). Ordering information is given on any current masthead page.

(34) Plaha, D.; Rogers, H. J. *Biochim. Biophys. Acta* **1983**, *760*, 246.
(35) Ecker, D. J.; Matzanke, B.; Raymond, K. N. *J. Bacteriol.* **1986**, *167*, 666.
(36) Shannon, R. D. *Acta Crystallogr., Sect. A* **1976**, *A32*, 751.